JACS
JOURNAL OF THE AMERICAN CHEMICAL SOCIETY

Article

pubs.acs.org/JACS

$AgNa(VO_2F_2)_2$: A Trioxovanadium Fluoride with Unconventional Electrochemical Properties

Martin D. Donakowski,[†] Arno Görne,[‡] John T. Vaughey,[§] and Kenneth R. Poeppelmeier*[,†]

[†]Department of Chemistry, Northwestern University, 2145 Sheridan Rd., Evanston, Illinois 60208-3113, United States

[‡]Institute of Inorganic Chemistry, RWTH Aachen University, Landoltweg 1, D-52074 Aachen, Germany

[§]Electrochemical Energy Storage Group, Chemical Sciences and Engineering Division, Argonne National Laboratory, Argonne, Illinois, 60439-4837, United States

Supporting Information

ABSTRACT: We present structural and electrochemical analyses of a new double-wolframite compound: $AgNa(VO_2F_2)_2$ or SSVOF. SSVOF is fully ordered and displays electrochemical characteristics that give insight into electrode design for energy storage beyond lithium-ion chemistries. The compound contains trioxovanadium fluoride octahedra that combine to form one-dimensional chain-like basic building units, characteristic of wolframite ($NaWO_4$). The 1D chains are stacked to create 2D layers; the cations Ag^+ and Na^+ lie between these layers. The vanadium oxide-fluoride octahedra are ordered by the use of cations (Ag^+, Na^+) that differ in polarizability. In the case of sodium-ion batteries, thermodynamically, the use of a sodium anode introduces a 300 mV loss in overall cell voltage as compared to a lithium anode; however, this can be counter-balanced by introduction of fluoride into the framework to raise the reduction potentials via an inductive effect. This allows sodium-ion batteries to have comparable voltages to lithium systems. With SSVOF as a baseline compound, we have identified new materials design rules for emerging sodium-ion systems that do not apply to lithium-ion systems. These strategies can be applied broadly to provide materials of interest for fundamental structural chemistry and appreciable voltages for sodium-ion electrochemistry.

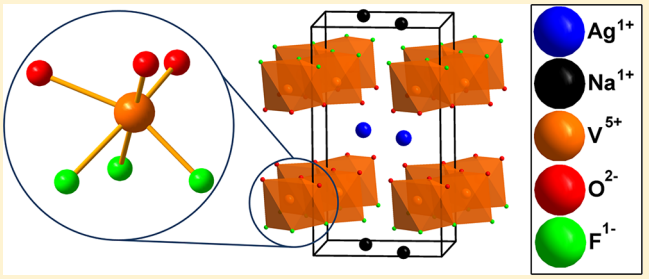

INTRODUCTION

To establish synthetic strategies to discover new materials for an electrochemical couple, several practical issues must be considered: theoretical capacity, fade rate, and cell voltage in addition to secondary issues such as materials costs. Research in solar, wind, hydropower, and other renewable energy sources continues to increase; thusly, grid level storage issues must be addressed to store excess energy for use at a later time. To date this has been studied with storage systems, such as Na/S, vanadium-redox, and banks of Li^+ ion batteries, where the desirable energy storage properties are possible, but their cost has not been adequately addressed.[1−4] Sodium ion batteries have been investigated as a low-cost alternative.[5,6] However, direct investigations to establish a suitable sodium-ion battery have not been sufficiently addressed. Previous research has typically explored optimization of current battery materials or translation of an established lithium-ion battery to a sodium-ion battery analogue. We demonstrate methodologies to create a sodium-ion battery with favorable characteristics. Specifically, a stable, layered material that provides an appreciable voltage in sodium electrochemistry and with a decreased ionic resistance. These efforts led to a new cathode material: $AgNa(VO_2F_2)_2$ (SSVOF). In this and related materials we have investigated the relationship between anion ordering, cation diffusion, and electrochemical properties to help establish design rules for sodium-ion battery cathodes. A synthetic strategy postulated for sodium-ion systems has been the addition of more ionic framework components, e.g., fluoride, to enlarge the HOMO−LUMO gap to offset the "toll" of moving away from lithium-based systems. Beyond sodium analogues of $LiFePO_4$ type systems, limited work has been published examining this concept.[5] Our results demonstrate the promise of fluorinated compounds for increased open circuit voltages with sodium-ion electrochemistry but highlight some of the difficulties including anion order-driven diffusion barriers, lower electronic conductivity, and stability in ionic electrolyte solutions.

Owing to their high-voltage potential, high-power/energy densities, and commonly layered topologies, vanadium oxide and vanadium oxide-fluoride compounds have been examined as cathode materials for many years. Examples of these materials include V_2O_5, $Ag_2V_4O_{11}$ (SVO), and $Ag_4V_2O_6F_2$ (SVOF).[7−16] $Ag_2V_4O_{11}$ has been the premier cathode material for the majority of implantable cardiac defibrillators (ICDs) owing to its capacity of over 300 mAh/g and fast rate of electronic discharge. The fluorinated material SVOF has superior behavior over SVO in terms of the reduction potential and a higher silver:vanadium ratio. In SVOF the fluoride

Received: April 26, 2013
Published: June 24, 2013

   dx.doi.org/10.1021/ja404189t | J. Am. Chem. Soc. 2013, 135, 9898−9906

incorporation raises the open circuit voltage. The layered structure facilitates good diffusion and movement of ions within the structure.

The use of a second metal cation to further stabilize a framework structure for ion insertion has been previously employed.[1,2,17] Within oxide-fluoride chemistry, a second metal can be used to drive the ordering of oxide and fluoride anions as understood by the use of hard and soft properties.[18−24] Multiple different (either chemically and/or crystallographically) cation sites inside an oxide-fluoride can be created using early transition metals that favor different bonding environments which decidedly order the anion sites as either an oxide or a fluoride anion coordination. This was recently demonstrated with syntheses of $Na_{1.5}Ag_{1.5}MO_3F_3$ (M = Mo, W); the sodium and silver ions differ sufficiently in their free ion polarizabilities to order the early transition metal oxide-fluorides.[20,23,25,26]

A three metal cation compound (consisting of cations with different polarizability and coordination preferences) would provide both structural stability and a driving force for oxide versus fluoride anion ordering; simultaneously, the fluoride anions would enhance the discharge voltage of the vanadium cations during the reduction process. With this knowledge in hand, we sought to use the hard−soft rules, recently employed by Fry et al., to hydrothermally synthesize sodium-silver vanadium oxide-fluoride materials.[23] We report the result of the syntheses: the compound $AgNa(VO_2F_2)_2$. To the best of our knowledge this material represents the first example of (i) an ordered trioxovanadium fluoride without organic ligands and (ii) an oxide fluoride derivative of a double wolframite structure. We believe the use of oxide-fluoride chemistry with varied metallic cations will result in new materials of importance to fundamental electrochemistry and structural inorganic chemistry and facilitate researchers to design sodium-ion battery cathode materials.

EXPERIMENTAL METHODS

Caution. Hydrofluoric acid is toxic and corrosive! It must be handled with extreme caution and appropriate protective gear and training.[27−29]

Materials. Vanadium oxide (V_2O_5, 99.6% min) was obtained from Alfa-Aesar, silver oxide (Ag_2O, 99%), lithium fluoride (LiF, 99%), sodium fluoride (NaF, 99%), and hydrofluoric acid (HF_{aq}, 49% in water, by weight) were obtained from Sigma Aldrich. Teflon film [fluoro-(ethylenepropylene), FEP] was obtained from American Durafilm. A battery grade electrolyte solution of 1.2 M $LiPF_6$ in 30/70 ethylcarbonate (EC) and ethyl methyl carbonate (EMC, solution ratio by weight) was purchased directly from Ube Industries (Japan). The same mixture of solvents (Ube) was used to make the 1.2 M $NaPF_6$ solution. Sodium foil was obtained from Sigma Aldrich, and lithium foil was obtained from FMC Lithium. The sodium foil was washed in the solvent mixture to remove any oils from packaging before use. All other materials were used as received.

Hydrothermal Syntheses. We hydrothermally synthesized the compound $AgNa(VO_2F_2)_2$ (SSVOF) by combining stoichiometric amounts of the metal reagents (1:1:2 Ag:Na:V) in a Teflon pouch: 0.2440 g of Ag_2O (2.106 mmol Ag^+), 0.0871 g (2.07 mmol Na^+) of NaF, and 0.3766 g (4.141 mmol V^{5+}) of V_2O_5 with 1.0 mL of 49% aqueous HF. The pouch was made by heat sealing Teflon film (FEP) as described previously.[18,30−32] The pouch was placed alone in a Teflon-lined 125 mL Parr autoclave with 42 mL of deionized water as backfill, heated at 150 °C for 24 h, cooled to 25 °C at a rate of 0.1 °C per minute, allowed to sit at room temperature for 48 h to allow further crystallization, opened in air, vacuum filtered, and allowed to dry for 48 h to recover 0.3116 g of SSVOF (0.8360 mmol, 40.38% yield in comparison to V_2O_5) of orange SSVOF crystals and powder; the platelet-like crystals were about 0.2 × 0.2 × 0.1 mm^3 in dimensions. HF_{aq} and water are known to permeate the Teflon film at high temperatures;[33] caution and proper disposal must be taken when handling the backfill and Teflon pouches. The pH of the reagent solution was about 2 before and after the reaction. The compound $AgLi(VO_2F_2)_2$ (SLVOF) was synthesized by combining 0.2472 g (2.133 mmol Ag^+) of Ag_2O, 0.0555 g (2.14 mmol Li^+) of LiF, and 0.3787 g (4.164 mmol V^{5+}) of V_2O_5 with 1.00 mL of 49% aqueous HF into a Teflon pouch. The pouch was then reacted in the same manner as for SSVOF to recover 0.1240 g of SLVOF (0.3476 mmol, 16.70% yield with respect to vanadium oxide). The platelet-like crystals were about 0.2 × 0.2 × 0.1 mm^3 in dimension. The pH of the reaction mixture was about 2 before and after the reactions.

To evaluate the composition space of sodium/silver vanadium oxide-fluoride compounds, we synthesized SSVOF with various mole fractions of $NaF:Ag_2O:V_2O_5$. These syntheses were performed with the procedure described above but with the use of 0.75 mL HF_{aq} and up to six pouches of varying reagent ratios within a Teflon-lined, 125 mL Parr acid digestion vessel that contained 45 mL of deionized water as backfill.

Reaction in Boiling HF_{aq}. Polycrystalline samples of SSVOF could also be synthesized at lower temperatures. We found that the reaction could be performed at 100 °C without hydrothermal conditions. The solid reagents were combined in stoichiometric ratios (9.0000 mmol V_2O_5, 4.4964 mmol Ag_2O, 8.9931 mmol NaF) with 3.00 mL HF_{aq} in a Teflon pouch that was submerged in a flask of boiling water. The pouch was allowed to sit at 100 °C for 3 h and then removed, allowed to cool to ambient temperature, and vacuum filtered in air to afford 1.8323g of SSVOF (4.9158 mmol, 54.62% yield in comparison to V_2O_5). In our previous studies of the compound $Ag_3VO_2F_4$, we found that crystallization could occur at higher temperatures (>25 °C) owing to a negative solubility constant.[34] We did not observe single crystals of SSVOF upon heating to 100 °C.

Room Temperature Synthesis. We previously have synthesized nanoparticulate needles of SVOF at room temperature with the use of HF_{aq};[15] analogously, we were able to create nanoparticulate needles of SSVOF. This was performed by combining 5.2081 g Ag_2O (22.474 mmol), 8.1646 g V_2O_5 (44.89 mmol), 1.8880 g Ag_2O (44.97 mmol), and 15 mL HF_{aq}. The pouch was agitated by hand, sealed with a thermal impulse sealer, and allowed to sit—undisturbed—for three weeks at ambient conditions (∼25 °C). The pouch was then opened in air, and the contents were vacuum filtered in air to yield 11.4420 g of nanoparticulate SSVOF (30.6977 mmol, 68.38% yield based on V_2O_5). PXRD was used to confirm the purity of the compound.

Crystallographic Determination. We mounted a single crystal of SSVOF or SLVOF on a glass fiber with paratone oil under a flow of nitrogen at 100 K. The single crystal XRD data were obtained with a Bruker Kappa APEX 2 CCD diffractometer with a detector-to-sample distance of 60 mm with monochromated Mo K_α radiation for SSVOF (λ = 0.71073 Å) and monochromated Cu K_α (λ = 1.54184). Copper radiation was used to obtain a higher signal of the low z ion Li^+; Cu K_α radiation has greater structure factors as compared to Mo K_α .The data were integrated with the SAINT-V7.23A program.[35] Absorption (numerical, face-indexed) corrections were applied to the data in the program XPREP for SSVOF; multiscan absorption corrections (SADABS) were applied to the data of SLVOF.[36,37] The structure of SSVOF was determined with XS within the Olex2 Suite;[37,38] direct methods were used to locate the positions of Ag^+ and V^{5+}. The remaining atomic positions were found within Fourier maps with the use of SHELXL within the Olex2 suite.[37,38] No additional symmetry or unit cells were found with PLATON.[39,40] We attempted to refine the Ag^+ and Na^+ sites as mixtures of Ag^+ and Na^+, but refinement showed complete order of the Ag^+ and Na^+ cations (the sites refined to fully Ag^+ or fully Na^+). SLVOF was solved by isostructural methods and refined. The crystallographic and acquisition parameters are displayed in Table 1.

Ion Exchange of SSVOF: Synthesis of $AgLi(VO_2F_2)_2$. Before electrochemical analysis was performed, we analyzed the compounds to determine if SSVOF was stable upon exposure to Li^+ electrolyte solutions. In two glass beakers we separately combined (i) 0.370 g

Table 1. Crystal Data and Structure Refinement for $AgNa(VO_2F_2)_2$ and $AgLi(VO_2F_2)_2$

compound	SSVOF	SLVOF
empirical formula	$AgNaV_2O_4F_4$	$AgLiV_2O_4F_4$
formula weight (au)	372.74	356.69
wavelength λ (Å)	0.71073	1.54184
space group	$P2/c$	$P2/c$
temperature (K)	100(2)	100(2)
a (Å)	10.3826(9)	9.9951(4)
b (Å)	5.8079(5)	5.6771(2)
c (Å)	4.9429(4)	4.8680(2)
β (°)	90.061(5)	90.596(2)
volume (Å^3)	298.06(5)	276.211(19)
calculated density (g/cm^3)	4.147	4.289
absorption coefficient μ (mm^{-1})	6.450	56.778
crystal size (mm^3)	0.26 × 0.10 × 0.05	0.19 × 0.03 × 0.02
independent reflections	877 [R_{int} = 0.0473]	470 [R_{int} = 0.0247]
completeness to θ	99.8% (θ = 30.03°)	96.5% (θ = 66.75°)
data/restraints/parameters	877/0/58	470/0/57
goodness-of-fit	0.952	1.192
final R indices [$>2\sigma(I)$][a]	R_{obs} = 0.0165, wR_{obs} = 0.0439	R_{obs} = 0.0199, wR_{obs}= 0.0539
R indices[a] (all data)	R_{all} = 0.0166, wR_{all} = 0.0440	R_{all} = 0.0200, wR_{all} = 0.0542
extinction coefficient	0.0105(14)	0.0062(6)

[a] $R = \Sigma||F_o| - |F_c||/\Sigma|F_o|$, $wR = (\Sigma[w(|F_o|^2 - |F_c|^2)^2]/\Sigma[w(|F_o|^4)])^{1/2}$, and for SSVOF: calc $w = 1/[\Sigma^2(F_o^2) + (0.0313P)^2 + 0.2493P]$, where $P = (F_o^2 + 2F_c^2)/3$. For SLVOF calc $w = 1/[\Sigma^2(F_o^2) + (0.0380P)^2 + 0.1939P]$, where $P = (F_o^2 + 2F_c^2)/3$.

$Li(NO_3)$, 0.100 g SSVOF and 10.0 mL hexanol and (ii) 0.0537 g SSVOF with 5.0 mL of hexanol. The beakers were stirred in ambient conditions for 24 h. The contents were then filtered and examined with EDX and PXRD. The control showed no modification of SSVOF; when SSVOF was exposed to $Li(NO_3)$, $AgLi(VO_2F_2)_2$ resulted (as determined by powder XRD and the presence of no signal from Na^+ ions within the EDX spectra, see Supporting Information).

To determine if this exchange would occur in the cell, we exposed SSVOF upon exposure to a Li^+-based electrolyte. Two laminates of SSVOF (a 1.6 cm^2 punch on aluminum metal) were made. One was allowed to sit under argon, the other laminate was soaked in a 1.2 M $LiPF_6$ EC/EMC (70/30 by volume) electrolyte solution for 15 days and dried. The two laminates were then evaluated by PXRD; we found no difference between the two laminates (see Supporting Information). The same experiment with a $NaPF_6$ EC/EMC electrolyte (exposed for 70 days) also showed no differences in the PXRD.

Electrochemical Characterization. Samples of SSVOF (hydrothermally prepared and nanoparticulate) were ground and combined into a slurry that contained 80% of the active material (hydrothermally prepared SSVOF or nanoparticulate SSVOF), 10% poly(vinlyidene difluoride) (PvDF) binder, and 10% acetylene black conductive additive. The mixtures were thoroughly mixed and laminated on an aluminum current collector and dried at 75 °C for 2 h to eliminate residual solvent. Electrochemical evaluations were performed using Hohsun 2032 (1.6 cm^2) cell hardware. Half cells were made in an argon atmosphere glovebox with lithium or sodium metal as the counter electrode, 1.2 M $LiPF_6$ (or 1.2 M $NaPF_6$) in EC/EMC (30/70 by weight) as an electrolyte solution, and Celgard 2325 separators. The cells were evaluated with a galvanostatic intermittent titration technique (GITT). Both sets of cells were discharged using 0.08 mA current for 15 min followed by a 3 h equilibration until the measured cell voltage reached 0.0 V. In order to evaluate the effect of diffusion length, nanoparticulate SSVOF was analyzed against a sodium anode, since previous studies had shown high ionic resistance, longer equilibrium times were needed. The cell was therefore measured with a discharge current of 0.08 mA for 30 min followed by a 6 h equilibration until the measured cell voltage reached 0.0 V.

Powder X-ray Diffraction. To ensure phase purity of the various samples of SSVOF, data were obtained with laboratory PXRD instruments at the Cohen Facility at Northwestern University and high-resolution synchrotron powder diffraction on beamline 11-BM at the Advanced Photon Source at Argonne National Laboratory. The high-resolution X-ray data of SSVOF showed no observable impurities. PXRD with laboratory X-ray instruments was additionally used to examine the products of the composition space of Ag_2O, NaF, and V_2O_5.

Pair Distribution Function. To compare the structure of nanoparticulate SSVOF versus hydrothermally prepared SSVOF, we obtained pair-distribution function (PDF) measurements on beamline 11-ID-B at the Advanced Photon Source of Argonne National Lab. TEM images showed that the nanoparticulate material consisted of needles that were ~50 nm in diameter and ~500 nm in length. Despite the anisotropy of the nanoparticulate SSVOF, the PDF diffractograms showed no significant difference between the crystal structures of the two synthetic products (see Supporting Information). Refinements of the PDF data were completed by use of X-ray crystallographic parameters and refinement.

RESULTS

Syntheses. The only compound within the Ag_2O/NaF/V_2O_5 system to incorporate all three metals was $AgNa(VO_2F_2)_2$. Figure 1 displays that at 150 °C SSVOF forms molar ranges of (1:2.00:28.5), (1:1.17:2.10), and (1:16.0:3.25) of Ag_2O:NaF:V_2O_5. The only trimetallic product formed in the reactions performed at room temperature, 100 °C, 150 °C, and 210 °C is the double-wolframite structure SSVOF and suggests that it is the energetic global minimum. High stability may be afforded by its structure and strong bonds formed between ions of similar polarizabilities.

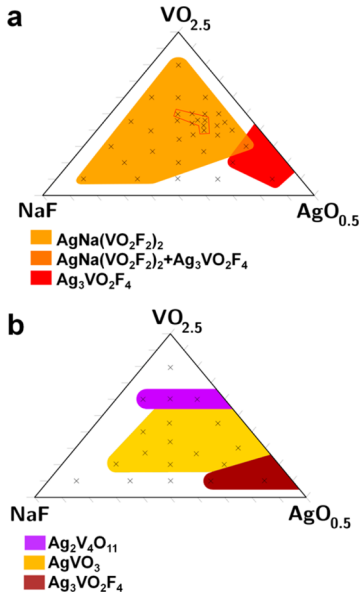

Figure 1. (a) Composition space diagram of the NaF:$VO_{2.5}$:$AgO_{0.5}$ system at 150 °C. The experiments were performed as described in the main text. The "x" indicates performed experiments, the red polygon outline indicates phase pure $AgNa(VO_2F_2)_2$, the legend provides the obtained phase at the specified concentration. The "x" in the white region indicates experimental observation of starting materials and/or $NaHF_2$. (b) Composition space diagram of the NaF:$VO_{2.5}$:$AgO_{0.5}$ system at 210 °C. No SSVOF was obtained at 210 °C.

dx.doi.org/10.1021/ja404189t | J. Am. Chem. Soc. 2013, 135, 9898−9906

We did observe, consistent with previous observations, that higher temperatures correlated with higher dimensionality of vanadium oxide (-fluoride) basic building units.[41,42] This is specific to the dimensionality of the vanadium oxide-fluoride basic buildings units and the condensation of these basic building units with other vanadium units. SSVOF consists of 1D units; when the same reagents are reacted at a higher temperature (210 °C), compounds of the same dimensionality of SSVOF (1D units: SVOF, $AgVO_3$) or of higher dimensionality (2D units, SVO) are formed. The 0D compound $Ag_3VO_2F_4$ synthesized at 150 °C contains an incommensurate structure and/or a disordered octahedra of V^{5+}.[34] The octahedra within $Ag_3VO_2F_4$ exist as a 0D basic building unit in a perovskite structure, separate from other vanadium oxide-fluoride units. In the case of $Ag_3VO_2F_4$ at reagent molar ratios (0.500:1:0.336) and (0.335:1:0.665) of V_2O_5:Ag_2O:NaF, the higher temperature is able to overcome the stabilizing energies of an incommensurate modulation and/or anion disorder to form an ordered, nonmodulated, higher dimensional vanadium oxide-fluoride unit.

For electrochemically active materials, layered topologies are highly desired as this allows intercalation of ions with maintenance of the structure. Discovery of new metal oxide/oxide fluorides should analyze the role of temperature upon synthesized products so as to obtain the desired (2D) geometry.

Figure 1 shows that SSVOF can be synthesized with a variety of initial loading compositions. The compositions at or near stoichiometric ratios resulted in phase-pure SSVOF. When the reagents were used in varied molar ratios, starting materials remained in the reaction and/or $NaHF_2$ was isolated as part of a product mixture. The use of NaF will alter the fluoride concentration of the HF_{aq} reactions, but the alternative use of Na_2O would alter the pH and would render reactions of high Na^+ concentrations nonacidic. To maintain the pH conditions, which can dramatically affect the synthesized product, we opted for the use NaF as a source for Na^+.

Spectroscopic Descriptions. To evaluate the 0D basic building unit within the 1D unit of trioxovanadium fluoride anions, we performed various spectroscopic analysis: NMR, FTIR, UV−vis-NIR, X-ray spectroscopies, (single crystal XRD, PXRD, PDF), energy dispersive analysis, and ICP-AES.

Each measurement (along with bond valence analysis to support elemental identity and order) was consistent with the bond distances listed in Table 3 and Supporting Information. ICP-AES confirmed the metallic ratios of SSVOF. PDF measurements further confirmed the structures and bond lengths and that these factors were equivalent if the material consisted of polycrystalline powder or nanoparticles. We performed ^{51}V MAS NMR and found the material to have a resonance of −388 (± 3) ppm. FTIR measurements of SSVOF show broad stretches in the V−O and V−F regions, consistent with multiple bending modes accessible to the low symmetry of the trioxovanadium fluoride octahedra (point group C_1) that is within the 1D chain unit. Qualitatively, the compound has an orange color similar to V_2O_5; UV−vis-NIR measurements showed that the compound has two absorptions at low, visible UV−vis regions (264 and 725 nm). The band gap of the material was determined to be 2.04 eV; for additional information on characterization, see Supporting Information.

Structural Description. The structure of SSVOF is an ordered double wolframite structure. Figure 2 illustrates the similarities of SSVOF with wolframite ($NiWO_4$) and the double wolframite structure (evidenced in $NaIn(WO_4)_2$). Other examples of double wolframites that contain sodium or silver include $NaB(WO_4)_2$ (B^{3+} = Fe, Ga, Sc) and $AgIn(WO_4)_2$.[43,44] As compared to the standard wolframite structure, the *a* axis is doubled for the double wolframite structure. Comparing the structure of SSVOF to $NaIn(WO_4)_2$, the W^{6+} cation is replaced by a V^{5+} cation, the In^{3+} cation is replaced by a Na^+ cation, and two O^{2-} anions are replaced by two F^- anions. The environment of each metal (Na^+, Ag^+, and V^{5+}) is within a distorted octahedron; the octahedron of V^{5+} is distorted by a second-order Jahn−Teller distortion.[45]

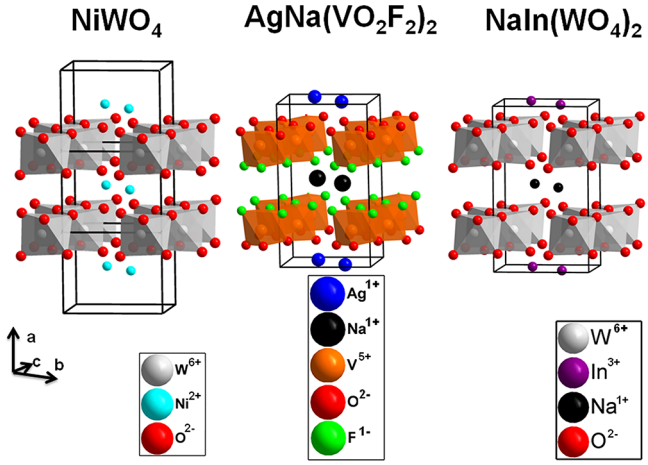

Figure 2. Comparison of the structure of wolframite ($NiWO_4$) and double wolframite ($NaIn(WO_4)_2$) structure types with SSVOF. The *a* axis of the wolframite structure is doubled as a consequence of the ordered Ag^+ and M^+ cations and O^{2-} and F^- anions to form the double wolframite structure. The structures of SSVOF, $NiWO_4$, and $AgIn(WO_4)_2$ contain octahedra of second-order Jahn−Teller distorted early transition metals. These edge-sharing octahedra are arranged in chains oriented along the *c* axis to make layers of the early transition metals. The ions coordinate based on similar polarizeabilities to form layers that consist of softer ions (Ag^+, O^{2-}) and harder ions (Na^+, F^-).

The octahedra are shown in Figure 3. The trioxovanadium fluoride 0D basic building units within the 1D unit have a particularly unusual geometry. To our knowledge, this is the first trioxovanadium fluoride octahedron without organic

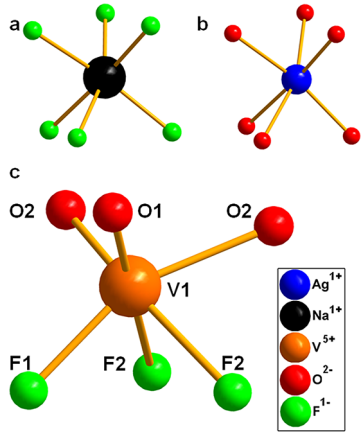

Figure 3. The octahedra within SSVOF. 1a) a distorted octahedron of sodium fluoride 1b) a distorted octahedron of silver oxide 1c) a Second-Order Jahn−Teller distorted octahedron of vanadium oxide-fluoride.

dx.doi.org/10.1021/ja404189t | J. Am. Chem. Soc. 2013, 135, 9898−9906

ligands. Previous trioxovanadium fluoride compounds with organic ligands are summarized in Table 2.[46−50] The vanadium

Table 2. Summary of Compounds with Trioxovanadium Fluoride Octahedra

compound	ref
$[H_3N(CH_2)_2NH_3]_2[V_6F_{12}(H_2O)_2\{O_3P(CH_2)_5PO_3\}_2\{HO_3P(CH_2)_5PO_3H\}]$	46
$[VOF_3(C_5H_5NO)_2] \cdot xH_2O$	47
$[VOF_3((C_5H_5)_3PO)_2]$	47
$[HN(C_2H_4)_3NH][V_2F_3O_2(O_3PC_6H_4PO_3H)]\cdot H_2O$	48
$[N(CH_2CH_2NH_3)_3]_2[NH_4][V_3O_2F_6(O_3PCH_2PO_3)_2]\cdot 2H_2O$	49
$[H_2N(C_2H_4)_2NH_2]_{1.5}[(VO)_3(AsO_4)F_4][VF_3(AsO_4)]\cdot 4H_2O$	50
$[C_6H_{13}N_2]_xV_{72}As_{24}O_{204}F_{54}\cdot nH_2O$	50
$AgNa(VO_2F_2)_2$	this work

oxide-fluoride octahedra contain two crystallographically distinct fluoride anions and two crystallographically distinct oxide anions. The vanadium is located on a general position, and the ions all have different bond lengths to the vanadium cation (point group C_1). The compound contains one vanadium oxide bond, 1.982(2) Å, that is longer than two of the vanadium fluoride bonds: 1.842(2) and 1.9563(19) Å. Typically, the vanadium oxide bonds are described as multiple bonds and vanadium fluoride bonds as single bonds.[51] The atypical bond lengths are stable owing to the anisotropic environment and the bond network of the double wolframite structure; the binding motif of the 1D vanadium oxide-fluoride units is shown in Figure 4.

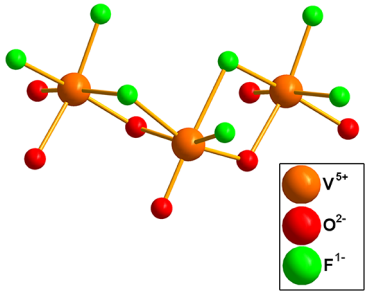

Figure 4. A portion of the $[VO_{1/1}O_{2/2}F_{1/1}F_{2/2}]_x$ chain; the vanadium cations are connected by symmetrically equivalent fluoride anions (F2) and symmetrically equivalent oxide anions (O2). The remaining oxide (O1) and fluoride anions (F1) are terminal and bond to silver and sodium cations, respectively.

To verify that anion order was in fact present within SSVOF, bond valence sum (BVS) calculations were performed. These BVS calculations are shown in Table 3. BVS calculations were applied for the other cations and anions and are described in the Supporting Information. The valences were consistent with an ordered material.

The sites of Ag^+ and Na^+ were also examined to see if there were mixed Ag^+_{1-x}/Na^+_x sites; no evidence for this was found (see Crystallographic Determination).

DISCUSSION

The electronic environment of $[VO_{3/1.5}F_{3/1.5}]^-$ is highly anisotropic. With regards to octahedra of early transition metals, our group has previously described the anionic basic building units of $[MoO_2F_4]^{2-}$ and $[VOF_5]^{2-}$ octahedra as cis directing in that they direct coordination through cis anions

Table 3. Bonding Distance and Bond Valence (BV) within the $[VO_{3/1.5}F_{3/1.5}]^{1-}$ Octahedra of $AgNa(VO_{3/1.5}F_{3/1.5})_2$

bond	length (Å)	BV[a]
V1−O1	1.6166(17)	1.655
V1−O2	1.7311(18)	1.214
V1−O2[b]	1.9839(16)	0.613
V1−F1	1.8398(15)	0.704
V1−F2	1.9543(15)	0.517
V1−F2[c]	2.1830(14)	0.278
BV sum[a]		4.962

[a]Details of calculations provided in Supporting Information. [b]Symmetry operation, x, $-y$, $z + 1/2$. [c]symmetry operation x, $-y$, $z - 1/2$.

owing to high residual valence on cis oriented anions. In contrast, the anionic basic building units $[WO_2F_4]^{2-}$, $[NbOF_5]^{2-}$, and $[TaOF_5]^{2-}$ are trans directing.[52−55]

Table 3 shows that four of the anions of the trioxovanadium fluoride octahedra are highly under bonded when only valence contributions of one vanadium octahedra are taken into account. For this reason, the two sets of bridging oxide and fluoride anions coordinate to another vanadium cation in a cis manner.

The trioxovanadium fluoride octahedra could thus be considered a 'cis and trans' director, as it coordinates in a cis manner to two metals that are trans to each other. This coordination of $[VO_{3/1.5}F_{3/1.5}]^{1-}$ to other vanadium oxide-fluoride anions is shown in Figure 4.

The sodium fluoride, silver oxide, and vanadium oxide-fluoride octahedra connect to other octahedra of the same element to generate edge-sharing, zigzag chain-like units (see Figure 5). Such zigzag chains are a feature of the wolframite and

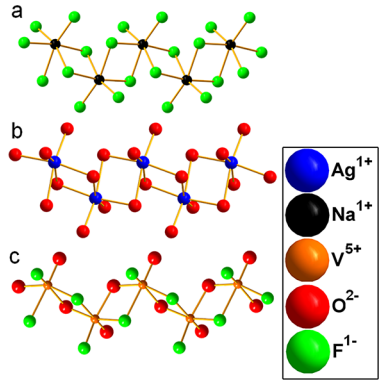

Figure 5. Edge-sharing zigzag chains of (a) 1D sodium fluoride units, (b) 1D silver oxide units, and (c) 1D trioxovanadium fluoride units. The sodium octahedra and the silver octahedra chains only connect to the vanadium oxide-fluoride chains (i.e., silver and sodium cations do not share anions). Each chain is connected to a total of four other chains of other elements.

double wolframite structures. Figure 2 shows that these 1D units 'stack' to form discrete regions of hard cations and anions (sodium and fluoride) and regions of soft cations and anions (silver and oxide). The trioxovanadium fluoride octahedra are oriented so that the soft anions (oxide) exist on one face of the octahedra and the fluoride anions are on the opposing face of the octahedra. We cannot decidedly state that cations order the anions or vice versa but rather that anisotropic environments

dx.doi.org/10.1021/ja404189t | J. Am. Chem. Soc. 2013, 135, 9898−9906

around oxide-fluoride polyhedra can favor order of anions/cations.

Owing to its layered structure (see Figure 2), SSVOF may undergo ion exchange upon exposure to concentrated salt or electrolyte solutions. We evaluated the electrochemical response of SSVOF as a cathode material. Before electrochemical analysis, we examined its stability in an electrochemical cell to check if ion exchange could occur with SSVOF. As determined by EDX spectroscopy, exposure of SSVOF to a 0.536 M $Li(NO_3)$ hexanol solution resulted in formation of $AgLi(VO_2F_2)_2$ at room temperature (EDX showed no Na^+ ions and PXRD showed maintenance of the structure). To verify this, we attempted the synthesis of a lithium derivative of SSVOF. We found that we could successfully obtain $AgLi(VO_2F_2)_2$ (SLVOF) by use of LiF instead NaF in the starting materials (see Syntheses).

It is possible, therefore for Li^+ to replace the Na^+ of SSVOF under mild conditions. Exposure of a laminated SSVOF sample to a $NaPF_6$ or $LiPF_6$/EC/EMC electrolyte solution did not noticeably modify the structure, see Supporting Information. This ion exchange may still occur in the electrochemical cells but would be difficult to observe owing to the difficulty in distinguishing between Na^+ and Li^+ in PXRD, particularly when the material is encased within a laminate matrix. This highlights the use of exchangeable cations in cathode materials. The structure of SLVOF, as evidenced by its preferential formation, is more stable than SSVOF, a process driven by the formation of Li−F bonds, which have a greater bond energy than Na−F: 141 kcal for LiF and 120 kcal for NaF.[56] Accordingly, the formation of an Li−F bond via ion exchange allows the disruption of an Na−F bond and possibly opens up diffusional pathways unavailable to the larger Na-based system as the volume of the octahedra does not change significantly with replacement by the much smaller lithium cation. Bonds, in this case Na−F, are unstable against high-molarity lithium salt solutions, which drives an ion exchange reaction yielding an electrochemically active compound from a near inactive one.

The electrochemical measurements may indicate ion exchange in the lithium-ion battery; the GITT experiments showed an initial voltage of ∼3.5 V but with a drop in voltage to 2.2 V (see Figure 6). This drop in voltage is consistent with the material's reducible elements being fully accessible. SSVOF provides an appreciable voltage for sodium-ion electrochemistry. In contrast to Figure 6, limited activity was observed in the battery of SSVOF with a sodium anode (see Figure 7).

Corresponding to theory and previous observations, the sodium battery had the expected 300 mV penalty; of note are the overpotentials of the system. Whereas the lithium battery showed relatively low overpotentials (∼100 mV) in the GITT study, the sodium battery showed very high overpotentials (>2 V).

Nanoparticulate SSVOF with the same crystallinity as hydrothermally prepared SSVOF was prepared. Figure 8 shows nanoparticulate SSVOF that was formed by synthesis at ambient conditions. Crystal strain induced by nanoparticle morphology could alter the crystallinity of SSVOF which may increase/decrease the ability for cations to intercalate during electrochemical use. Pair-distribution function data were obtained at Argonne National Lab to examine if there were significant differences of the nanoparticulate crystallinity compared to the hydrothermally prepared SSVOF. We obtained good fitness with refinement of unit cell parameters only. The structures remained largely unchanged; the unit cell

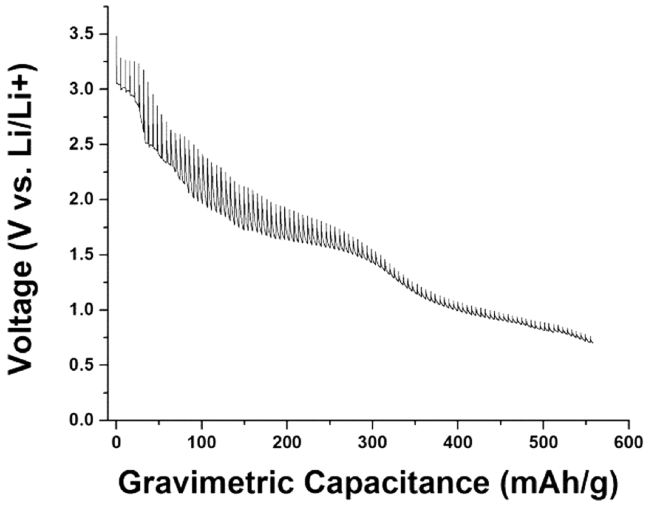

Figure 6. Galvanostatic intermittent titration technique curve illustrating the discharge behavior of SSVOF with a lithium anode. The battery cell begins at a voltage of ∼3.5 V, typical for vanadium oxide fluorides. The cell quickly decreases to 2 V before 200 mAh/g with an unsteady voltage. We attribute this discharge primarily to the conversion of Ag^+ to silver metal and V^{5+} to V^{4+}, but the overlapping processes make interpretation difficult. The subsequent discharge of the material is attributed to reduction of V^{4+} to V^{3+} and V^{2+}. The steep decreases in the voltage indicate decreased integrity of the material so that the material's components are electrochemically fully accessible.

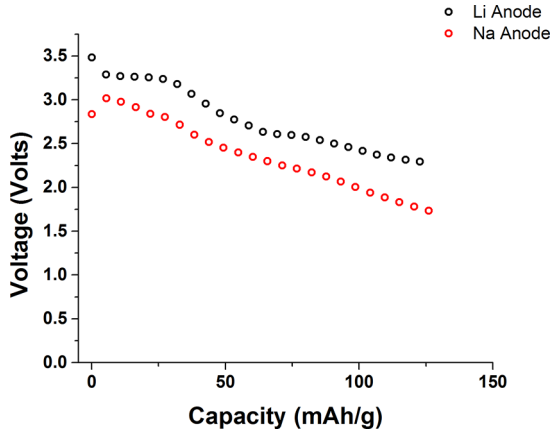

Figure 7. GITT experiment of hydrothermally prepared SSVOF as a cathodic material against lithium (lithium-ion battery) and sodium (sodium-ion battery) anodes. The sodium anode shows decreased voltage as compared to the lithium anode but has a comparable voltage as compared to unfluorinated vanadium cathodes, such as $Ag_2V_4O_{11}$ (SVO). The data are plotted only in the range of capacitance available before the sodium anode SSVOF shorted. The voltages are in respect to their sodium or lithium anodes.

volume of each structure only differed by about 0.5 Å^3. This is due most likely to the 'large' size of the particles; the particles measure ∼50 × 500 nm.

This needle-shaped morphology has previously been observed for the compound SVO.[57] We were unable to obtain high-quality TEM images (Figure 8) owing to sample degradation during electron microscopy. During microscopy, spherical particles were observed. We attribute this to reduction of Ag^+ to metallic silver while under an electron beam.[15] As the crystallinity is the same with nanoparticulate or hydrothermally synthesized SSVOF, comparisons of their electrochemistry

dx.doi.org/10.1021/ja404189t | J. Am. Chem. Soc. 2013, 135, 9898−9906

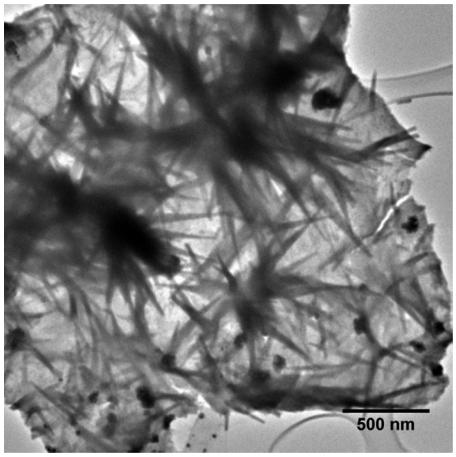

Figure 8. Transmission electron microscope (TEM) image of the nanoparticulate SSVOF synthesized at room temperature. During acquisition, the electron beam degraded the sample while the sample was under vacuum. This resulted in the spherical particles shown in the image that we attribute to reduced silver that was removed from the structure. The needles of SSVOF measure ~50 nm in diameter by 500 nm in length.

would examine the effect of the size/surface area of the material.

Figure 9 shows the sodium-ion cell was found to have a discharge voltage of about 3.0 V with very high impedance. To reduce the impedance of the sodium-ion battery of SSVOF, we synthesized nanoparticulate SSVOF (Figure 8) to decrease the diffusion distances. These materials show the decreased impedance and a more stable discharge when compared to micrometer-sized SSVOF.

SSVOF within a sodium-ion battery cell: nanoparticulate cathodes of oxide-fluoride materials can allow (i) increased open circuit voltage compared to pure oxide materials and (ii) decreased impedance as compared to macroscopic cathode materials. Comparison of the over potentials of the sodium anode batteries is shown in Figure 9 for nanoparticulate and hydrothermally prepared SSVOF.

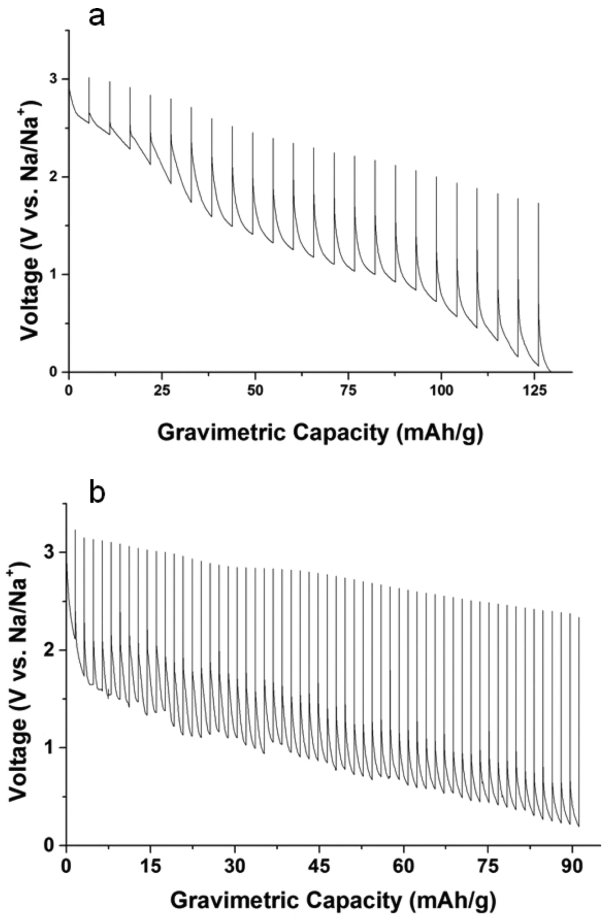

Figure 9. (a) GITT experiment of the discharge behavior of hydrothermally prepared SSVOF against a sodium anode. (b) GITT experiment of the discharge behavior of nanoparticulate SSVOF. Note that the two compounds have different ranges of gravimetric capacity owing to different voltage cutoffs (when the voltage was zero and shorted the device). The nanoparticulate SSVOF exhibits a lower impedance and more steady voltage obtained with hydrothermally prepared SSVOF; however, the 'higher' voltage is an artifact as the system had not yet reached equilibrium despite allowing 6 h between measurements.

CONCLUSION

We have synthesized an ordered vanadium oxide-fluoride compound with the structure of a double-wolframite, $AgNa(VO_2F_2)_2$. The compound contains trioxovanadium fluoride octahedra within 1D basic building units. The material can be synthesized at a multitude of reactant ratios and temperatures in good yield. We are optimistic that room temperature syntheses of this—and previous materials—can result in nanoparticle morphologies when synthesized with HF_{aq}. Electrochemically, the material displays favorable voltage for sodium-ion batteries and lowered resistance when synthesized as a nanoparticulate material. The use of oxide-fluoride chemistry can result in early transition metal oxide-fluoride geometries to expand upon fundamental structures. Design strategies for sodium-ion cathodes should be established upon (i) use of fluorinated materials to raise voltage potentials and offset the penalty of use of a sodium anode in place of a lithium anode; (ii) use of polarizability matching to create layers and ordered oxide-halide/sulfide materials; (iii) choice of framework cations that can facilitate intercalation of anodic cations; (iv) multi-anion networks to create a electrochemically stable framework; (v) temperature control to synthesize layered materials; and (vi) nanoparticulate syntheses to decrease ionic resistance. These generalized principles are promising for new and interesting compounds in fundamental and electrochemical studies. More attention is necessary to establish ionic networks that can increase ionic mobility, such as weaker ionic bond frameworks, and maintain a stable structure within an electrochemical cell.

ASSOCIATED CONTENT

Supporting Information

FTIR and UV−vis-NIR, V^{51} solid-state MAS NMR, PDF, and ICP-AES spectroscopies of SSVOF and/or SLVOF; BVS calculations; tables (S1−S18) of crystal data of $AgNa(VO_2F_2)_2$and $AgLi(VO_2F_2)_2$ (atomic coordinates, anisotropic displacement parameters, bond lengths, and bond angles), unit cells for PDF fits of nanoparticulate $AgNa(VO_2F_2)_2$ and hydrothermally prepared SSVOF at 298 K, FTIR and UV−vis-NIR spectra fitting parameters of $AgNa(VO_2F_2)_2$, ICP-AES results for SSVOF, BVS calculations for cations and anions of $AgNa(VO_2F_2)_2$ and $AgLi(VO_2F_2)_2$, Figures S1−S13 of FTIR and UV−vis-NIR spectra and corresponding fits, V^{51} MAS

dx.doi.org/10.1021/ja404189t | J. Am. Chem. Soc. 2013, 135, 9898−9906

NMR spectra, PXRD patterns of hydrothermally prepared SSVOF with synchrotron radiation, a PXRD pattern of $AgNa(VO_2F_2)_2$ formed at 100 °C, a PXRD pattern of nanoparticulate $AgNa(VO_2F_2)_2$, a PXRD pattern of $AgLi(VO_2F_2)_2$, PDF fits of hydrothermally prepared $AgNa(VO_2F_2)_2$ and nanoparticulate SSVOF, and CIFs of $AgNa(VO_2F_2)_2$ and $AgLi(VO_2F_2)_2$. This material is available free of charge via the Internet at http://pubs.acs.org.

AUTHOR INFORMATION

Corresponding Author

krp@northwestern.edu

Notes

The authors declare no competing financial interest.

ACKNOWLEDGMENTS

This work was supported by a grant from the National Science Foundation (Solid State Chemistry award no. DMR-1005827). Solid-state NMR was obtained at IMSERC at Northwestern University on an instrument obtained with a grant from the NSF (award no. DMR-0521267). PXRD patterns were obtained on instruments supported by the MRSEC program of the National Science Foundation (award no. DMR-0520513). Use of the Advanced Photon Source at Argonne National Laboratory was supported by the U.S. Department of Energy, Office of Science, Office of Basic Energy Sciences, under contract no. DE-AC02-06CH11357. J.T.V. would like to acknowledge support from the Batteries for Advanced Transportation Technologies (BATT) Program, U.S. Department of Energy under contract no. DE-AC02-06CH11357.

We would like to thank Karena Chapman and Kevin Beyer (Argonne National Lab, ANL), for assistance with PDF measurements, Matt Suchomel (ANL) for assistance with PXRD diffraction, Yuyuan Lin (Northwestern University, NU) for TEM imaging, Michael Holland (NU) for single crystal XRD collection, single crystal X-RAY, ICP-AES, and FTIR measurements were performed at IMSERC at NU which is supported with grants from NSF-NSEC, NSF-MRSEC, the Keck Foundation, the state of Illinois, and NU. We thank Amy Sarjeant (NU) and Charlotte Stern (NU) for helpful discussions in regards to the crystal structures. Solid-state NMR spectra were obtained with assistance of Yuyang Wu (NU). TEM data were obtained at the EPIC center at NU; Diffuse-reflectance spectra were obtained at the Keck Biophysics Facility at NU, which is supported by grants from the W. M. Keck Foundation, NU, the NIH, the Rice Foundation, and the Robert H. Lurie Comprehensive Cancer center. Table formatting was performed with CIFTool software (unpublished) written by Christos Malliakas (NU).

REFERENCES

(1) Scrosati, B.; Selvaggi, A.; Croce, F.; Gang, W. *J. Power Sources* **1988**, *24*, 287−294.

(2) Selvaggi, A.; Croce, F.; Scrosati, B. *J. Power Sources* **1990**, *32*, 389−396.

(3) Goodenough, J. B.; Kim, Y. *Chem. Mater.* **2009**, *22*, 587−603.

(4) Liao, Y.; Park, K.-S.; Xiao, P.; Henkelman, G.; Li, W.; Goodenough, J. B. *Chem. Mater.* **2013**, *25*, 1699−1705.

(5) Ong, S. P.; Chevrier, V. L.; Hautier, G.; Jain, A.; Moore, C.; Kim, S.; Ma, X.; Ceder, G. *Energy Environ. Sci.* **2011**, *4*, 3680−3688.

(6) Doeff, M. M.; Shirpour, M.; Cabana, J. Meeting Abstracts. In Proceedings of The Electrochemical Society (MA2012-02);Honolulu, Hawaii; October 7-12, 2012; The Electrochemical Society: Pennington, New Jersey, 2012; p 1831.

(7) Liang, C. C.; Bolster, M. E.; Murphy, R. M. U.S. Patent 4,310,609, July 5, 1983, 1982.

(8) Liang, C. C.; Bolster, M. E.; Murphy, R. M. U.S. Patent 4,391,729, July 5, 1983, 1983.

(9) Takeuchi, E. S.; Piliero, P. *J. Power Sources* **1987**, *21*, 133−141.

(10) García-Alvarado, F.; Tarascon, J. M. *Solid State Ionics* **1994**, *73*, 247−254.

(11) Takeuchi, K. J.; Marschilok, A. C.; Davis, S. M.; Leising, R. A.; Takeuchi, E. S. *Coord. Chem. Rev.* **2001**, *219−221*, 283−310.

(12) Crespi, A. M.; Somdahl, S. K.; Schmidt, C. L.; Skarstad, P. M. *J. Power Sources* **2001**, *96*, 33−38.

(13) Sorensen, E. M.; Izumi, H. K.; Vaughey, J. T.; Stern, C. L.; Poeppelmeier, K. R. *J. Am. Chem. Soc.* **2005**, *127*, 6347−6352.

(14) Sauvage, F. d. r.; Bodenez, V.; Vezin, H.; Albrecht, T. A.; Tarascon, J.-M.; Poeppelmeier, K. R. *Inorg. Chem.* **2008**, *47*, 8464−8472.

(15) Albrecht, T. A.; Sauvage, F.; Bodenez, V.; Tarascon, J. M.; Poeppelmeier, K. R. *Chem. Mater.* **2009**, *21*, 3017−3020.

(16) Sauvage, F.; Bodenez, V.; Vezin, H.; Morcrette, M.; Tarascon, J. M.; Poeppelmeier, K. R. *J. Power Sources* **2010**, *195*, 1195−1201.

(17) Zhang, F.; Whittingham, M. S. *Electrochem. Commun.* **2000**, *2*, 69−71.

(18) Norquist, A. J.; Heier, K. R.; Stern, C. L.; Poeppelmeier, K. R. *Inorg. Chem.* **1998**, *37*, 6495−6501.

(19) Marvel, M. R.; Lesage, J.; Baek, J.; Halasyamani, P. S.; Stern, C. L.; Poeppelmeier, K. R. *J. Am. Chem. Soc.* **2007**, *129*, 13963−13969.

(20) Marvel, M. R.; Pinlac, R. A. F.; Lesage, J.; Stern, C. L.; Poeppelmeier, K. R. *Z. Anorg. Allg. Chem.* **2009**, *635*, 869−877.

(21) Aldous, D. W.; Lightfoot, P. *Solid State Sci.* **2009**, *11*, 315−319.

(22) Pinlac, R. A. F.; Stern, C. L.; Poeppelmeier, K. R. *Crystals* **2011**, *1*, 3−14.

(23) Fry, A. M.; Seibel, H. A.; Lokuhewa, I. N.; Woodward, P. M. *J. Am. Chem. Soc.* **2011**, *134*, 2621−2625.

(24) Donakowski, M. D.; Vinokur, A. I.; Poeppelmeier, K. R. *Z. Anorg. Allg. Chem.* **2012**, *638*, 1991−1995.

(25) Pearson, R. G. *Chemical Hardness*; John Wiley & Sons, Inc.: New York, 1997.

(26) Shannon, R. D.; Fischer, R. X. *Phys. Rev. B* **2006**, *73*, 235111.

(27) Bertolini, J. C. *J. Emerg. Med.* **1992**, *10*, 163−168.

(28) Peters, D.; Miethchen, R. *J. Fluorine Chem.* **1996**, *79*, 161−165.

(29) Segal, E. B. *Chem. Health Saf.* **2000**, *7*, 18−23.

(30) Harrison, W. T. A.; Nenoff, T. M.; Gier, T. E.; Stucky, G. D. *Inorg. Chem.* **1993**, *32*, 2437−2441.

(31) Halasyamani, P.; Willis, M. J.; Stern, C. L.; Poeppelmeier, K. R. *Inorg. Chem.* **1996**, *35*, 1367−71.

(32) Halasyamani, P. S.; Heier, K. R.; Norquist, A. J.; Stern, C. L.; Poeppelmeier, K. R. *Inorg. Chem.* **1998**, *37*, 369−371.

(33) Chamberlain, J. M. Ph.D. Dissertation, Northwestern University; Evanston, IL, 2010.

(34) Chamberlain, J. M.; Albrecht, T. A.; Lesage, J.; Sauvage, F. d. r.; Stern, C. L.; Poeppelmeier, K. R. *Cryst. Growth Des.* **2010**, *10*, 4868−4873.

(35) *SAINT*, v7.23A in Bruker APEX v2.1-0, 7.23A; Bruker AXS Inst. Inc.: Madison, WI, 2005.

(36) Sheldrick, G. *SADABS*; University of Göttingen: Göttingen, Germany, 1996.

(37) Sheldrick, G. *Acta Crystallogr., Sect. A* **2008**, *64*, 112−122.

(38) Dolomanov, O. V.; Bourhis, L. J.; Gildea, R. J.; Howard, J. A. K.; Puschmann, H. *J. Appl. Crystallogr.* **2009**, *42*, 339−341.

(39) Spek, A. *Acta Crystallogr., Sect. D* **2009**, *65*, 148−155.

(40) Spek, A. L. *PLATON*; Utrecht University: Utrecht, The Netherlands, 2001.

(41) Aldous, D. W.; Stephens, N. F.; Lightfoot, P. *Dalton Trans.* **2007**, 4207−4213.

(42) Bhattacharya, S.; Ramanujachary, K. V.; Lofland, S. E.; Magdaleno, T.; Natarajan, S. *CrystEngComm* **2012**, *14*, 4323−4334.

(43) Klevtsov, P. V.; Klevtsova, R. F. *J. Solid State Chem.* **1970**, *2*, 278−282.
(44) Sorokina, O. V.; Karpov, V. N.; Dzhurinskii, B. F.; Pashkova, A. V. *Neorg. Mater.* **1976**, *12*, 2202−2205.
(45) Pearson, R. G. *Proc. Natl. Acad. Sci. U.S.A.* **1975**, *72*, 2104−2106.
(46) Ouellette, W.; Yu, M. H.; O'Connor, C. J.; Zubieta, J. *Inorg. Chem.* **2006**, *45*, 7628−7641.
(47) Davis, M. F.; Levason, W.; Paterson, J.; Reid, G.; Webster, M. *Eur. J. Inorg. Chem.* **2008**, *2008*, 802−811.
(48) DeBurgomaster, P.; Liu, H.; Ouellette, W.; O'Connor, C. J.; Zubieta, J. *Inorg. Chim. Acta* **2010**, *363*, 4065−4073.
(49) Smith, T. M.; Tichenor, M.; Vargas, J. M.; O'Connor, C. J.; Zubieta, J. *Inorg. Chim. Acta* **2011**, *378*, 250−256.
(50) Kotsapa, E.; Weller, M. T. *Chem. Commun. (Cambridge, U. K.)* **2011**, *47*, 6132−6134.
(51) Ballhausen, C. J.; Gray, H. B. *Inorg. Chem.* **1962**, *1*, 111−122.
(52) Heier, K. R.; Norquist, A. J.; Halasyamani, P. S.; Duarte, A.; Stern, C. L.; Poeppelmeier, K. R. *Inorg. Chem.* **1999**, *38*, 762−767.
(53) Welk, M. E.; Norquist, A. J.; Stern, C. L.; Poeppelmeier, K. R. *Inorg. Chem.* **2000**, *39*, 3946−3947.
(54) Welk, M. E.; Norquist, A. J.; Stern, C. L.; Poeppelmeier, K. R. *Inorg. Chem.* **2001**, *40*, 5479−5480.
(55) Izumi, H. K.; Kirsch, J. E.; Stern, C. L.; Poeppelmeier, K. R. *Inorg. Chem.* **2005**, *44*, 884−895.
(56) Page, F. M.; Sugden, T. M. *Nature* **1959**, *183*, 1672.
(57) Sauvage, F.; Bodenez, V.; Tarascon, J.-M.; Poeppelmeier, K. R. *J. Am. Chem. Soc.* **2010**, *132*, 6778−6782.